

A New Structural Type in Ternary Chalcogenide Chemistry: Structure and Properties of $\text{Nb}_2\text{Pd}_3\text{Se}_8$

DOUGLAS A. KESZLER AND JAMES A. IBERS

Department of Chemistry, Northwestern University, Evanston, Illinois 60201

Received June 20, 1983; in revised form October 14, 1983

A study of the Nb-Pd-Se system has afforded a new phase, $\text{Nb}_2\text{Pd}_3\text{Se}_8$. The structure of this phase has been established through single-crystal X-ray measurements. The compound crystallizes in space group D_{2h}^2 -*Pbam* with two formula units in a cell of dimensions $a = 15.074(6)$, $b = 10.573(4)$, $c = 3.547(2)$ Å. In this unusual structure there are two chains of edge-sharing selenium trigonal prisms centered by niobium atoms. These chains conjoin through two types of palladium atoms—square planar and square pyramidal—each coordinated by selenium atoms. As a consequence of this conjunction tunnels extending along c result. Electrical conductivity measurements indicate that this material is a metallic-semiconductor.

Introduction

As a continuation of our interest in the structural and crystal chemistry of Group VIII B (Pt group) chalcogenides and oxides (1) and ternary chalcogenides in general (2), we have discovered a new phase in the Nb-Pd-Se system.

The investigation of phase behavior in systems of the type TM -Pd-Se, where TM = Group IV B-Group VIII B transition metal, has been largely neglected. Indeed, the only reports on TM -Pd-Se systems have concerned the formation at high pressure of phases, $M_x\text{Pd}_{1-x}\text{Se}_2$ ($M = \text{Co, Ni, Ru, Rh}$); $x \geq 0.3$ (3), with the pyrite structure.

In contrast, numerous studies of TM -Nb-Se materials, prompted chiefly by observations of interesting and often unusual electrical and magnetic properties, have been reported. These reports have detailed the characterization of two extensive ternary

(quaternary) families of compounds: $M_x\text{NbSe}_2$ ($M = \text{Ti, V, Cr, Mn, Fe, Co, Ni, Rh}$); $x < 0.33$ (4, 5) and $MM'\text{Nb}_2\text{Se}_{10}$ ($M = \text{Fe, V, Cr}$; $M' = \text{Fe, V, Cr, Nb}$) (6-8).

For the series $M_x\text{NbSe}_2$ the ternary atom, M , occupies tetrahedral or octahedral sites in the van der Waals' gap between slabs consisting of sheets of Nb atoms bonded to and sandwiched between two layers of chalcogens. The environment of the Nb atoms is trigonal prismatic so the NbSe_2 sublattice may be viewed as a two-dimensional array of edge-sharing Se trigonal prisms occupied by Nb atoms. These structural features are emphasized in Fig. 1. This low-dimensional structural nature is retained for the $MM'\text{Nb}_2\text{Se}_{10}$ series of compounds. These materials consist of infinite NbSe_3 chains linked by edge-sharing Se octahedra centered by the $M(M')$ atom(s). An NbSe_3 chain is sketched in Fig. 2.

Until the present study, for phases prepared at ambient pressure the structural

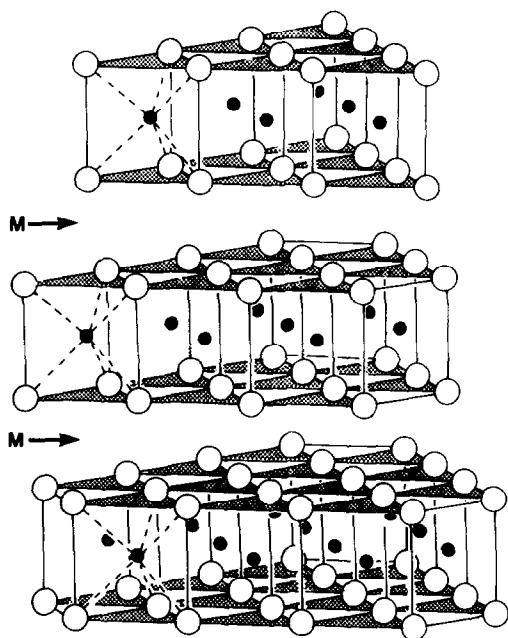


FIG. 1. Schematic representation of $M_x\text{NbSe}_2$ compounds.

chemistry of Pd^{2+} has been dominated by square-planar coordination of Pd by chalcogen (9). One might well speculate that the synthesis of a Nb/Pd/Se compound would produce a material with a new structural type as the aforementioned Nb-Se sublattices are maintained because the steric demands of the ternary atom, M , are readily met by the type and number of available sites. In this way we have prepared and characterized the new material, $\text{Nb}_2\text{Pd}_3\text{Se}_8$.

Experimental

A combination of the elements, Nb powder (99.99%, Johnson-Matthey), Pd powder (99.9%, Alfa), and Se pellets (99.999%, Atomergic), was loaded into a silica tube. The tube was evacuated to $\sim 10^{-5}$ Torr and then bromine ($\sim 2 \text{ mg/cm}^3$ of tube volume) was added. The vessel was sealed and placed for 3 weeks in a tube furnace having a temperature gradient of $650\text{--}600^\circ\text{C}$. Small

needle-shaped crystals formed at the hot end of the tube.

A chemical analysis was performed with the electron microprobe of an EDAX equipped Cambridge S-4 scanning electron microscope, with mixtures of NbSe_2 and PdSe_2 as standards. Intensities were corrected and the chemical composition was obtained from the computer program MAGICIV (10). The variation in composition within individual crystals and among several crystals was within experimental error. Analysis of the crystal used for the structure determination (vide infra) afforded the composition: Nb 17.35, Pd, 26.95, Se, 55.70%; calcd. for $\text{Nb}_2\text{Pd}_3\text{Se}_8$: Nb, 16.35, Pd, 28.08, Se, 55.57%.

Four-probe single-crystal conductivity measurements were made along c , the needle axis, following procedures described previously (11).

The compound $\text{Nb}_2\text{Pd}_3\text{Se}_8$ was subjected to a single-crystal X-ray study. The systematic extinctions ($0kl, k = 2n + 1; h0l, h = 2n + 1$) and the symmetry of the intensity-weighted reciprocal lattice, as determined from Weissenberg and precession photographs, were indicative of the orthorhombic space groups $D_{2h}^2\text{-Pbam}$ and $C_{2v}^3\text{-Pba}2$. As a satisfactory residual index obtains

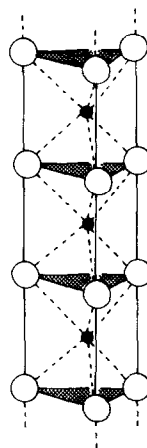


FIG. 2. Schematic representation of NbSe_3 chains.

TABLE I
CRYSTAL DATA AND INTENSITY COLLECTION FOR Nb₂Pd₃Se₈

Mol. wt.	1136.69
Space group	D_{2h}^2 - <i>Pbam</i>
<i>a</i> , Å	15.074(6)
<i>b</i> , Å	10.573(4)
<i>c</i> , Å	3.547(2)
<i>V</i> , Å ³	565
<i>Z</i>	2
<i>T</i> of data collection, K ^a	115
Crystal vol., mm ³	0.000075
Radiation	graphite monochromatized MoK α ($\lambda(K\alpha_1) = 0.7093$ Å)
Linear abs. coeff., cm ⁻¹	320
Transmission factors	0.585–0.698
Detector aperture	3.7 mm wide, 4.4 mm high 32 cm from crystal
Takeoff angle, deg.	3.2
Scan speed, deg. min ⁻¹	2.0 in 2 θ
$\lambda^{-1} \sin \theta$, limits, Å ⁻¹	0.0276–1.0142 2.25° \leq 2 θ (MoK α_1) \leq 92.0°
Background counts	10 sec at each end of scan with rescan option ^b
Scan range, deg.	1.0 below K α_1 to 1.1 above K α_2
Data collected	<i>h, k</i> \pm <i>l</i>
ρ factor	0.04
No. unique data (including $F_0^2 < 0$)	2717
No. unique data with $F_0^2 > 3\sigma(F_0^2)$	1418
$R(F^2)$	0.106
$R_w(F^2)$	0.123
R (on F for $F_0^2 > 3\sigma(F_0^2)$)	0.049
Error in observation of unit wt., e ²	0.99

^a The low-temperature system is based on a design by Huffman, J. C., Ph.D. thesis, Indiana University, 1974.

^b The diffractometer was operated under the Vanderbilt disk oriented system (P. G. Lenhert, *J. Appl. Crystallogr.* **8**, 568–570 (1975).)

from averaging the two octants of data, the former space group is favored. Diffraction data were collected from a cylindrical crystal bathed in a N₂-cold stream on a Picker FACS-1 diffractometer in a manner standard for this laboratory (12). Six standard reflections measured at 100-reflection intervals showed no significant variation in intensity during the course of data collection. Inspection of electron photomicrographs of the cylindrical crystal revealed no discernible crystal edges. For the absorption correction the shape of the crystal was therefore approximated by 22 equally separated lon-

gitudinal faces capped by faces of the form {001}. Crystal data and crystallographic details are provided in Table I.

All calculations were performed on a Harris 800 computer with programs standard in this laboratory. Conventional atomic scattering factors (13) were used and anomalous dispersion corrections (14) were applied to each atom with use of values $\Delta f'$ and $\Delta f''$ from Cromer and Waber (13). The structure was solved by direct methods (MULTAN80). An E map revealed the positions of all the atoms. A suitable model for refinement was derived from

TABLE II
POSITIONAL PARAMETERS FOR Nb₂Pd₃Se₈

Atom	Wyckoff notation	Site symmetry	x	y	z
Nb	4h	m	0.115914(54)	0.215325(75)	1/2
Pd(1)	2a	2/m	0	0	0
Pd(2)	4g	m	0.216161(44)	0.381202(64)	0
Se(1)	4g	m	0.988913(61)	0.231846(90)	0
Se(2)	4g	m	0.157342(60)	0.043908(86)	0
Se(3)	4h	m	0.283350(61)	0.250324(91)	1/2
Se(4)	4h	m	0.115622(64)	0.457417(88)	1/2

TABLE III
ANISOTROPIC THERMAL PARAMETERS^a FOR Nb₂Pd₃Se₈

	β_{11}	β_{22}	β_{33}	β_{12}
Nb	0.000299(23)	0.000756(48)	0.00431(42)	-0.000049(28)
Pd(1)	0.000228(27)	0.000958(61)	0.01043(59)	-0.000048(32)
Pd(2)	0.000309(18)	0.000782(38)	0.00447(34)	-0.000024(24)
Se(1)	0.000280(27)	0.001132(64)	0.00532(51)	-0.000007(32)
Se(2)	0.000283(26)	0.000672(55)	0.00621(50)	0.000061(32)
Se(3)	0.000289(27)	0.001079(55)	0.00580(49)	-0.000031(33)
Se(4)	0.000481(28)	0.000829(57)	0.00601(50)	0.000065(34)

$$^a e^{-\beta_{11}h^2 + \beta_{22}k^2 + \beta_{33}l^2 + 2\beta_{12}hk}$$

an examination of a drawing of the contents of the unit cell. The two octants of data were averaged and final anisotropic least-squares refinement on F_o^2 for 2717 unique data resulted in residuals $R = 0.106$ and $R_w = 0.123$. The final difference electron density map revealed no features $>2\%$ of the height of a Pd atom.

The following results are tabulated: positional parameters (Table II), anisotropic thermal parameters (Table III), and structure amplitudes (Table S-I).¹

Description of the Structure and Discussion

The structure of Nb₂Pd₃Se₈ is described in terms of bond distances and angles in Table IV. A stereoview of the structure is furnished in Fig. 3. The labeling scheme is provided in Fig. 4. The structure consists of a framework of fibers extending along c .

¹ See NAPS document No. 04138 for 11 pages of supplementary material. Order from ASIS/NAPS, Microfiche Publications, P.O. Box 3513, Grand Central Station, New York, NY 10163. Remit in advance \$4.00 for microfiche copy or for photocopy, \$7.75 up to 20 pages plus \$0.30 for each additional page. All orders must be prepaid. Institutions and organizations may order by purchase order. However, there is a billing and handling charge for this service of \$15. Foreign orders add \$4.50 for postage and handling, for the first 20 pages, and \$1.00 for additional 10 pages of material. Remit \$1.50 for postage of any microfiche orders.

The fibers are composed of two chains of edge-sharing Se trigonal prisms centered by Nb atoms and bridged by Pd atoms bound to four coplanar Se atoms (Fig. 5). The chains are further capped by additional Pd atoms located above the square faces formed by adjoining Se trigonal prisms. As illustrated in Fig. 4, the full nature of the three-dimensional structure is realized with linkage of *trans*-Se atoms of the square plane of each unit and the capping Pd atoms of additional chains. As a consequence of this connectivity the Se atoms about this Pd atom impart a square-pyramidal environment to the Pd atom. This framework further necessitates the formation of channels parallel to c with vacant octahedral and tetrahedral sites (Fig. 4).

TABLE IV
SELECTED BOND DISTANCES (Å) AND ANGLES (deg.) FOR Nb₂Pd₃Se₈

Nb-2Se(1)	2.616(1)		
Nb-2Se(2)	2.612(1)	Se(1)-Nb-Se(2)	76.19(4)
Nb-Se(3)	2.551(2)	Se(1)-Nb-Se(4)	86.12(4)
Nb-Se(4)	2.559(2)	Se(1)-Nb-Se(1)	85.35(6)
Nb-2Pd(1)	3.374(1)	Se(3)-Nb-Se(4)	81.76(5)
Nb-2Pd(2)	2.916(1)		
Nb-2Nb	3.546(2)		
Pd(1)-2Se(1)	2.457(2)		
Pd(1)-2Se(2)	2.417(2)	Se(1)-Pd(1)-Se(2)	82.87(4)
Pd(1)-2Pd(1)	3.546(2)		
Pd(2)-Se(2)	2.567(2)	Se(3)-Pd(2)-Se(3)	91.92(6)
Pd(2)-2Se(3)	2.467(1)	Se(3)-Pd(2)-Se(4)	85.34(4)
Pd(2)-2Se(4)	2.468(1)	Se(2)-Pd(2)-Se(3)	94.06(5)
Pd(2)-2Pd(2)	3.546(2)		

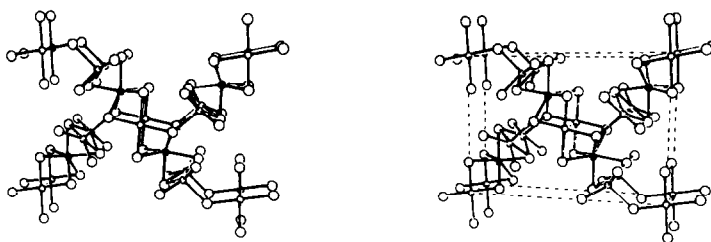


FIG. 3. Stereoview of the structure of $\text{Nb}_2\text{Pd}_3\text{Se}_8$. Nb are small filled circles; Pd are small open circles; Se are large open circles.

The Nb–Se distances² range from 2.551(2) to 2.616(1) Å and the average, 2.60(3) Å, is comparable with that observed in NbSe_2 , 2.595(2) Å (15). The selenium trigonal prism is not exactly regular. The triangular face, Se(4)–Se(1)–Se(4), approximates an isosceles triangle with dimensions 3.533(2) and 3.547(2) Å. The triangular face, Se(2)–Se(3)–Se(2), is more distorted with dimensions 3.394(2) and 3.547(2) Å. These faces are not exactly parallel; the dihedral angle between them is 177.69(5)°.

The Pd(1)–Se distances are consistent with those observed in other structures with Se atoms bound to Pd atoms in a square-planar manner. The Se square plane shortens along the edge shared with the trigonal prism with the resultant acute angle 82.87(4)° for Se(1)–Pd(1)–Se(2).

The average Pd(2)–Se distance, 2.467(1) Å, in the basal plane of the square pyramid is somewhat shorter than the Pd(2)–Se(2) (apex) distance, 2.567(2) Å. The distortions of the basal plane are reflected by the angles Se(3)–Pd(2)–Se(3), 91.92(6)° and Se(3)–Pd(2)–Se(4), 85.34(4)°. The Pd atom lies 0.383(1) Å above the basal plane. Insofar as we know, this is the first time a chalcogenic square-pyramidal coordination has been clearly established for a Group VIII B platinum-group metal in an inorganic solid-state compound.

² An estimated standard deviation in parentheses is the larger of that estimated for a single observation from the inverse matrix or from the values averaged.

The geometric distortions about the metal atoms are consistent with the chemical inequivalence of the Se atoms (Table IV). Each Se atom is bound to three metal atoms, with the exception of atom Se(2) which bridges two Pd atoms and two Nb atoms. The Se–Se distances within a chain range from 3.226(2) to 3.574(2) Å. The crys-

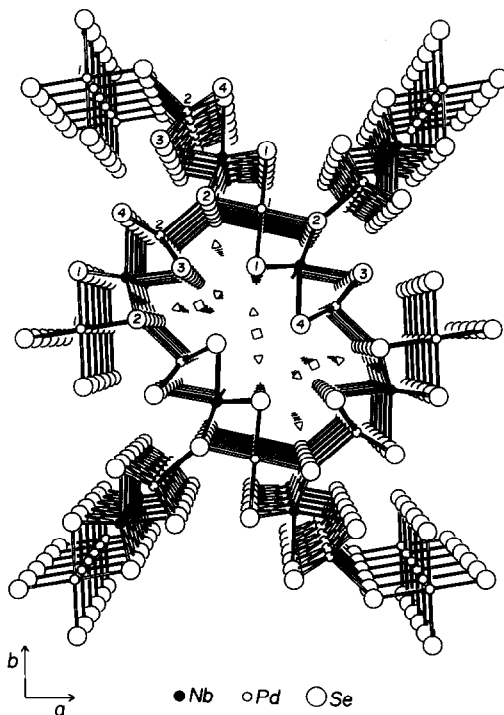


FIG. 4. Perspective view down [001], showing the labeling scheme. Δ —Vacant tetrahedral sites; \square —vacant octahedral sites.

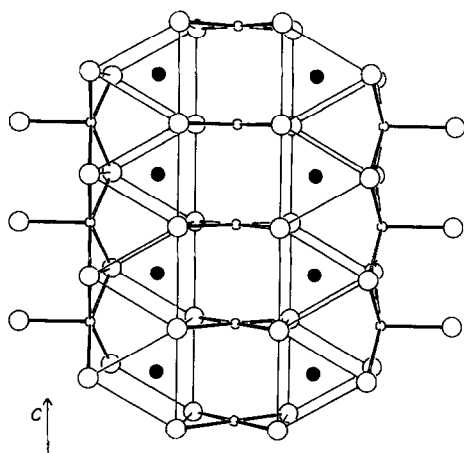


FIG. 5. Individual chain in $\text{Nb}_2\text{Pd}_3\text{Se}_8$ as viewed along b . Nb are small filled circles; Pd are small open circles; Se are large open circles.

tal radius of Se is 1.84 \AA (16). The $\text{Se} \cdots \text{Se}$ distances across the channel range from $3.574(2)$ to $4.052(2) \text{ \AA}$. These values are comparable with the $\text{Se} \cdots \text{Se}$ distance across the van der Waals' gap of NbSe_2 , $3.550(4)$ (15), and similar interactions in NbSe_3 (17), $3.73(1)$ – $4.17(1)$. The \triangle -Se and \square -Se distances (Fig. 4) range from 1.95 to 2.45 \AA and from 2.47 to 2.84 \AA , respectively.

The temperature dependence of the sin-

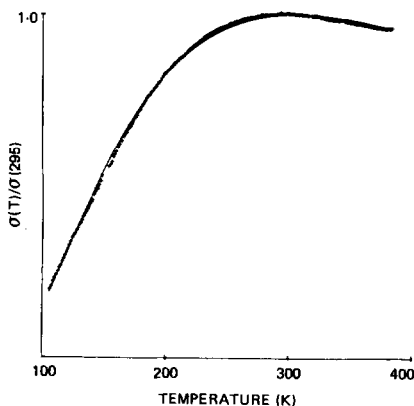


FIG. 6. Temperature dependence of the single-crystal conductivity along the needle axis c for $\text{Nb}_2\text{Pd}_3\text{Se}_8$ (observed + + +; calculated —).

gle-crystal conductivity in the region 380 – 100 K is illustrated in Fig. 6. The conductivity attains a maximum of $6.6 \text{ ohm}^{-1} \text{ cm}^{-1}$ at 295 K before falling as the temperature is lowered. This temperature dependence of the conductivity for $\text{Nb}_2\text{Pd}_3\text{Se}_8$ is similar to that observed for low-dimensional materials such as $\text{K}_2\text{Pt}(\text{CN})_4\text{Br}_{0.3} \cdot 3\text{H}_2\text{O}$ (18) and N -methylphenazium tetracyanoquinodimethanide (19). Epstein and Conwell have presented the relation $\sigma(T) = AT^{-\alpha} \exp(-\Delta/T)$ that has been used in fitting the temperature dependence of the conductivity for such materials (19). A least-squares fit of the data in Fig. 6 affords $A = 3.12 \times 10^5 \text{ ohm}^{-1} \text{ cm}^{-1} \text{ K}^\alpha$, $\alpha = 1.60$, and $\Delta = 486.89 \text{ K}$ for the $\text{Nb}_2\text{Pd}_3\text{Se}_8$ crystal and satisfactorily reproduces the conductivity over the complete temperature region.³ As discussed by Epstein and Conwell the preexponential term may be ascribed to a temperature-dependent mobility and the Boltzmann term to the activated generation of charge carriers in a narrow band gap semiconductor. From this interpretation the compound $\text{Nb}_2\text{Pd}_3\text{Se}_8$ is classified as a metallic-semiconductor (20).

Consistent with the crystallographic and electrical conductivity results a simple formal valence description for the compound $\text{Nb}_2\text{Pd}_3\text{Se}_8$ is Nb^{5+} , Pd^{2+} , Se^{2-} . As may be expected for $d^0 \text{ Nb}^V$ and $d^8 \text{ Pd}^{II}$, the material exhibits semiconducting behavior, although the magnitude of the band gap is suggestive of a high degree of covalency. Indeed the occurrence of trigonal-prismatic coordination for the Nb atom attests to this covalency (21).

Acknowledgments

We thank J. Martinsen for assistance with the electrical conductivity measurement. We are indebted to the Northwestern University Materials Research Center for the use of their scanning electron microscope facility.

³ The data are fit with an error of less than 1% based on the rms deviation calculated from the fit.

References

1. (a) D. CAHEN, J. A. IBERS, AND R. D. SHANNON, *Inorg. Chem.* **11**, 2311 (1972); (b) D. CAHEN, J. A. IBERS, AND M. H. MUELLER, *ibid.*, **13**, 110 (1974); (c) D. CAHEN, J. A. IBERS, AND J. B. WAGNER, JR., *ibid.*, **13**, 1377 (1974).
2. A. GLEIZES, J. REVELLI, AND J. A. IBERS, *J. Solid State Chem.* **17**, 363 (1976).
3. (a) D. AVIGNANT, D. CARRÉ, R. COLLINS, AND A. WOLD, *Mater. Res. Bull.* **14**, 553 (1979). (b) D. CARRÉ, D. AVIGNANT, R. C. COLLINS, AND A. WOLD, *Inorg. Chem.* **18**, 1370 (1979).
4. A. R. BEAL, in "Physics and Chemistry of Materials with Layered Structures" (F. Lévy, Ed.), Vol. 6, p. 251, Reidel, Dordrecht (1979).
5. (a) S. S. P. PARKIN AND R. H. FRIEND, *Philos. Mag. B* **41**, 65 (1980); *ibid.*, p. 95; (b) S. S. P. PARKIN AND A. R. BEAL, *Philos. Mag. B* **42**, 627 (1980).
6. S. J. HILLENUS, R. V. COLEMAN, R. M. FLEMING, AND R. J. CAVA, *Phys. Rev. B* **23**, 1567 (1981).
7. (a) R. J. CAVA, V. L. HIMES, A. D. MIGHELL, AND R. S. ROTH, *Phys. Rev. B* **24**, 3634 (1981); (b) A. MEERSCHAUT, P. GRESSIER, L. GUEMAS, AND J. ROUXEL, *Mater. Res. Bull.* **16**, 1035 (1981).
8. A. BEN SALEM, A. MEERSCHAUT, L. GUEMAS, AND J. ROUXEL, *Mater. Res. Bull.* **17**, 1071 (1982).
9. (a) Powder Data File, Card No. 18-953. Joint Committee on Powder Diffraction Standards, Swarthmore, Pa.; (b) W. BRONGER, J. EYCK, W. RÜDORFF, AND A. STÖSSEL, *Z. Anorg. Allg. Chem.* **375**, 1 (1970); (c) W. BRONGER AND J. HUSTER, *J. Less-Common Met.* **23**, 67 (1971); (d) W. BRONGER, in "Physics and Chemistry of Materials with Layered Structures" (F. Lévy, Ed.) Vol. 2, p. 93, Reidel, Dordrecht (1979).
10. J. W. COLBY, *Advan. X-Ray Anal.* **11**, 287 (1968).
11. T. E. PHILLIPS, R. P. SCARINGE, B. M. HOFFMAN, AND J. A. IBERS, *J. Amer. Chem. Soc.* **102**, 3435 (1980).
12. J. M. WATERS AND J. A. IBERS, *Inorg. Chem.* **16**, 3273 (1977).
13. D. T. CROMER AND J. T. WABER, "International Tables for X-Ray Crystallography," Vol. IV, Table 2.2A; D. T. CROMER, Table 2.3.1, Kynoch Press, Birmingham, England (1974).
14. J. A. IBERS AND W. C. HAMILTON, *Acta Crystallogr.* **17**, 781 (1964).
15. M. MAREZIO, P. D. DERNIER, A. MENTH, AND G. W. HULL, JR., *J. Solid State Chem.* **4**, 425 (1972).
16. R. D. SHANNON, *Acta Crystallogr. Sect. A* **32**, 751 (1976).
17. J. L. HODEAU, M. MAREZIO, C. ROUCAU, R. AYROLES, A. MEERSCHAUT, J. ROUXEL, AND P. MONCEAU, *J. Phys. C* **11**, 4117 (1978).
18. J. S. MILLER AND A. J. EPSTEIN, "Progress in Inorganic Chemistry" (S. J. Lippard, Ed.), Vol. 20, p. 1, Interscience, New York (1976).
19. A. J. EPSTEIN, E. M. CONWELL, D. J. SANDMAN, AND J. S. MILLER, *Solid State Commun.* **23**, 355 (1977).
20. A. J. EPSTEIN, "Molecular Metals", (W. E. Hatfield, Ed.), p. 155, Plenum, New York (1979).
21. R. HUISMAN, R. DE JONGE, C. HAAS, AND F. JELLINEK, *J. Solid State Chem.* **3**, 56 (1971).